(33) Hoffmann, R. *Tetrahedron Lett.* **1970**, 2907. Günther, H. *ibid.* **1970**, 5173.
(34) Dewar, M. J. S.; Haddon, R. C.; Komornicki, A.; Rzepa, H. *J. Am. Chem. Soc.* **1977**, *99*, 377.
(35) Loew, L. M.; Wilcox, C. F. *J. Am. Chem. Soc.* **1975**, *97*, 2296.
(36) LeBel, N. A.; Spurlock, L. A. *Tetrahedron* **1964**, *20*, 215.
(37) Yoneda, S.; Yoshida, Z.; Winstein, S. *Tetrahedron* **1972**, *28*, 2395. Lustgarten, R. K.; Brookhart, M.; Winstein, S. *J. Am. Chem. Soc.*, **1972**, *94*, 2347.
(38) Jefford, C. W.; Burger, U. *Chimia* **1970**, *24*, 385.
(39) Schleyer, P. v. R.; Blanchard, K. R.; Woody, C. D. *J. Am. Chem. Soc.* **1963**, *85*, 1358.

Chemically Derivatized n-Type Silicon Photoelectrodes. Stabilization to Surface Corrosion in Aqueous Electrolyte Solutions and Mediation of Oxidation Reactions by Surface-Attached Electroactive Ferrocene Reagents

Jeffrey M. Bolts, Andrew B. Bocarsly, Michael C. Palazzotto, Erick G. Walton, Nathan S. Lewis, and Mark S. Wrighton*

Contribution from the Department of Chemistry, Massachusetts Institute of Technology, Cambridge, Massachusetts 02139. *Received August 17, 1978*

Abstract: Derivatization of n-type Si photoelectrode surfaces with (1,1′-ferrocenediyl)dichlorosilane results in the persistent attachment of photoelectroactive ferrocene species. Derivatized surfaces have been characterized by cyclic voltammetry in EtOH or H_2O electrolyte solutions. Such surfaces exhibit persistent oxidation and reduction waves, but the oxidation requires illumination as expected for an n-type semiconductor. The oxidation wave is observed at potentials ~300 mV more negative than at Pt, reflecting the ability to oxidize ferrocene contrathermodynamically by irradiation. Derivatized n-type Si can be used to sustain the oxidation of solution-dissolved ferrocene under conditions where "naked" Si is incapable of doing so. Further, derivatized n-type Si has been used in an aqueous electrolyte to oxidize $Fe(CN)_6^{4-}$. Finally, the photooxidation of solution species has been demonstrated to occur via photogeneration of holes in the Si, oxidation of the surface-attached species, and then oxidation of the solution species by the surface-attached oxidant, providing the first direct proof of mediated electron transfer for any derivatized electrode. Derivatized electrodes can be used to sustain the conversion of light to electricity but the efficiencies are low. Based on results for 632.8-nm irradiation, solar energy conversion efficiencies of ~1% can be obtained.

We describe herein proof-of-concept experiments illustrating that deleterious photoanodic decomposition of n-type Si photoelectrodes can be substantially suppressed by chemical derivatization of the surface using a hydrolytically unstable ferrocene derivative. With the knowledge that all n-type semiconducting materials are susceptible to photoanodic decomposition,[1,2] we regard this problem as one of the real impediments to the exploitation of semiconductor/liquid junction cells in energy conversion and photoelectrosynthesis. Further, we describe results which serve to prove that oxidation reactions at the illuminated electrode interface can be mediated by the surface-attached electroactive species. By *mediated* we mean that the surface-attached electroactive molecule is first oxidized and it then oxidizes a solution species (Scheme I). Owing to the rectifying properties of a semiconductor electrode, the mediation experiments described herein are uniquely doable at the semiconductor electrodes. Our demonstration of mediated electron transfer establishes the viability of endowing photosensitive electrodes with molecular specific properties.

In an earlier communication[3] we showed that (1,1′-ferrocenediyl)dichlorosilane can derivatize the surface of n-type Si. The resulting surface exhibits persistent photoelectroactivity in that the surface-attached ferrocene species can be repetitively cycled between its oxidized and reduced form by linearly sweeping the illuminated electrode cyclically between −0.6 and +0.4 vs. a saturated calomel reference electrode (SCE). Importantly, the photooxidation of the attached ferrocene species can be effected at contrathermodynamic potentials. By this we mean that the attached species can be oxidized at an electrode potential where the attached species thermodynamically should remain in the reduced form (vide infra). This fact, along with the relatively durable surface, reveals that it should be possible to oxidize certain solution species at contrathermodynamic potentials. In particular, any solution reductant which is oxidizable with the oxidized form of the surface-attached species should be oxidizable by illumination of the derivatized electrode. Our objective is to take advantage of the light absorption and charge-separating properties of the semiconductor, while exploiting the redox properties of the surface-bound molecule. Others have attempted to exploit the light absorption properties of covalently attached dye molecules on SnO_2[4] or adsorbed species on other photostable oxides,[5] in order to extend the wavelength response of large band gap semiconductor photoelectrodes.

Scheme II shows the interface energetics[6a] for an illuminated "naked" (nonderivatized) photoelectrode compared to the derivatized case where the position of the electrode potential (E_f), top of the valence band (E_{VB}), bottom of the conduction band (E_{CB}), redox level of the attached species ($E(A^+/A)$), and the solution species ($E(B^+/B)$) are given relative to a reference electrode. We assume here that the values of E_{CB} and E_{VB} remain fixed for any value of E_f and that E_{CB} and E_{VB} are the same for the naked and derivatized surface. The stimuli of light and potential in Scheme I can be specified as being light energy great enough ($\geq E_{BG}$) to excite electrons from the valence band to the conduction band, and an electrode potential more positive than E_{CB} such that there is sufficient band bending to kinetically inhibit reduction of A^+ or B^+ for E_f more negative than $E(B^+/B)$. It is photogenerated hole formation in the valence band that allows contrathermodynamic oxidations, but the band bending in-

0002-7863/79/1501-1378$01.00/0

Scheme I. Pictorial Representation of Mediated Oxidation of Solution Species B Where A Is the Electrode-Attached Electroactive Species

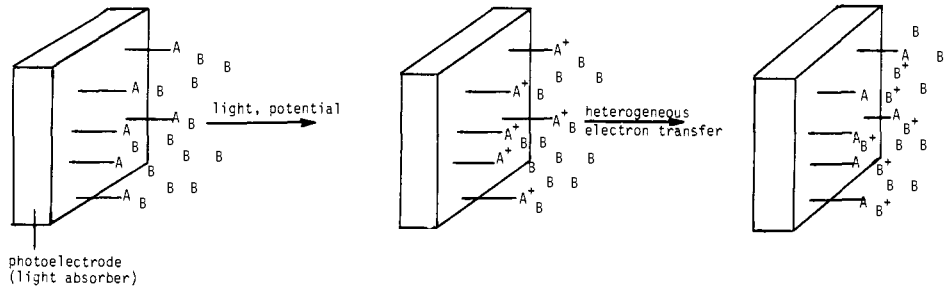

Scheme II. Interface Energetics for a Naked Semiconductor and a Derivatized Semiconductor Exposed to an Electrolyte Solution Containing the B^+/B Couple[a]

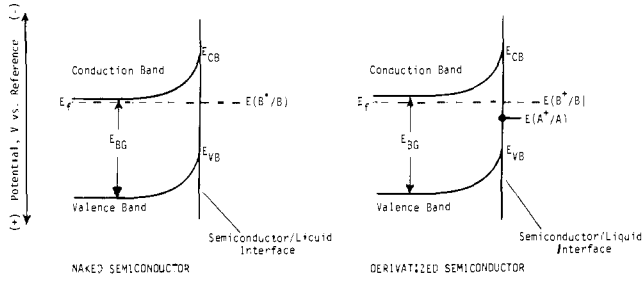

[a] The situation is for an illuminated electrode ($>E_{BG}$) at short circuit; note that the attached A^+/A potential need not be pinned to E_f under photoexcitation conditions.

Scheme III. Photoinduced Oxidation of B to B^+ at Electrode Potential, E_f, Where B^+ Could Be Thermodynamically Reduced to B[a]

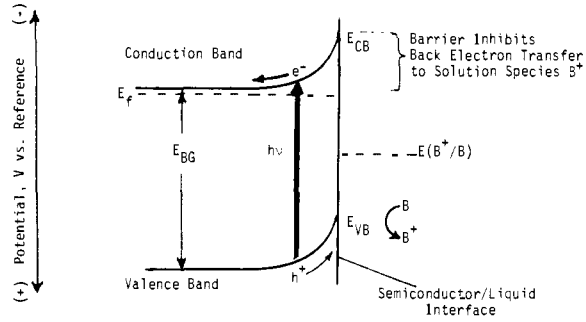

[a] Reduction is kinetically inhibited by the barrier to electron transfer associated with band bending.

hibits back electron transfer (Scheme III). The assumption that the interface energetics are not altered by derivatization of the photoelectrode leads to the conclusion that the theoretical efficiency of an optical to chemical or electrical energy conversion is unchanged by derivatization. The energy conversion efficiency is governed by the quantum efficiency for net electron flow and the extent to which the oxidation of B can be effected contrathermodynamically.

The presence of the electroactive, surface-attached species may substantively alter the mechanism of the net oxidation of solution species B in such a way as to lend specificity to the oxidation. Perhaps more important for now is that the surface derivatization can alter the kinetics for the net interfacial processes. In the case of n-type Si, the specific objective in altering kinetics is to reduce the current efficiency for the growth of insulating SiO_x on the surface and improve the current efficiency for the net interfacial oxidation of a solution species.

In the experiments described herein we set out to establish that (1) a chemically derivatized n-type Si surface could be used to effect the photooxidation of solution species under conditions where the naked surface is incapable of doing so and (2) oxidation of the solution species at the derivatized electrode occurs via photogenerated hole formation in the semiconductor, oxidation of the surface-attached molecule, and finally oxidation of the solution species by the surface-attached oxidant. With respect to the first point, the critical problem concerns the growth of SiO_x on the electrode with the oxygen presumably originating from H_2O in the solvent. Consequently, the new results described below relate to experimentation aimed at stabilizing the surface in the presence of H_2O. Cyclic voltammetry and equilibrium current-potential curves have been used to characterize naked compared to derivatized surfaces, in order to establish aspects of the interfacial charge transfer kinetics and energetics.

Results and Discussion

A. Cyclic Voltammetry for "Naked" Si in EtOH Solutions of Ferrocene. Work in this laboratory established that ferrocene can be oxidized with ~100% current efficiency at illuminated n-type Si in EtOH solutions of $[n\text{-}Bu_4N]ClO_4$:[6b]

$$\text{ferrocene} \xrightarrow[h\nu,\ \text{n-type Si}]{-e^-} \text{ferricenium (photoanode)} \quad (1)$$

Our earlier work was carried out at a fairly high ferrocene concentration ($>5 \times 10^{-2}$ M) in order to ensure that ferricenium formation would successfully compete with any SiO_x formation:

$$Si \xrightarrow[x(H_2O)]{-(2x)e^-} SiO_x + (2x)H^+ \quad (2)$$

When the EtOH solution is sufficiently free of H_2O, cyclic voltammetry can be used to characterize the interfacial electron transfer chemistry of ferrocene at n-type Si. Figure 1a shows representative cyclic voltammograms of a naked, HF-etched, n-type Si photoelectrode. The ferrocene concentration is low, 6.1×10^{-4} M, and a diffusion-limited photooxidation current is observed for quiet solutions with a peak at +0.2 V vs. SCE. Stirred solutions usually give a hole (light intensity) limited current which is proportional to light intensity. As we reported earlier for n-type Si, no oxidation current obtains in the dark. This fact is consistent with the conclusion that the oxidation of ferrocene occurs via hole generation in the valence band upon photoexcitation with band gap or greater energy light. On the cathodic sweep reduction of the ferricenium occurs and gives a peak for the reduction current. The position of the reduction peak depends on whether the light is on or off; when the light is on there is an anodic current at potentials more positive than approximately −0.2 V vs. SCE, but in the dark there is no anodic current to compete with the reduction current and the reduction peak is consequentially at a more anodic potential.

The thermodynamic potential, $E°$, for the ferricenium/ferrocene couple is +0.45 V vs. SCE.[7] The observation of the photoanodic peak at +0.2 V vs. SCE shows that ferrocene can be oxidized at contrathermodynamic potentials at the irradiated n-type Si. The onset of the photoanodic current in the

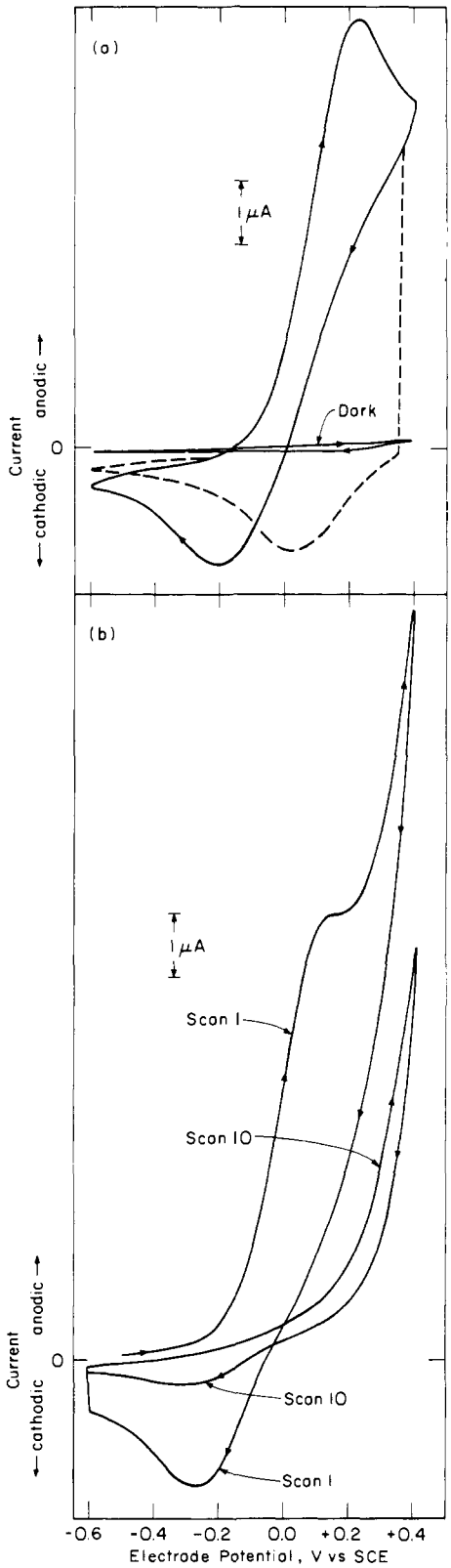

Figure 1. Effect of H_2O on ability of n-Si to sustain the photooxidation of ferrocene. Illumination refers to uniform (beam expanded) irradiation from a He-Ne laser (632.8 nm). In (a) cyclic voltammograms are shown for n-type Si in 6.1×10^{-4} M ferrocene/0.1 M $[n\text{-}Bu_4N]ClO_4$ in EtOH solvent scanning from −0.6 to +0.4 V vs. SCE at 100 mV/s. One scan is shown for total darkness; the smooth curves shows four repetitive scans with illumination showing penwidth reproducibility with an anodic peak at ~+0.2 V and a cathodic peak at ~−0.1 V. Where the dashed curve begins (+0.4 V) the illumination was blocked and the reduction peak is still observable though at a somewhat more anodic position (~+0.05 V). In (b) we show scans 1 and 10 after adding Ar-purged, distilled H_2O. Except for the presence of the ~6.9 M H_2O everything is the same as in (a) with illumination. The scans between 1 and 10 show progressive deleterious changes and are omitted for clarity.

cyclic voltammogram is in accord with the previously measured[6b] maximum open-circuit photopotential of an n-type Si-based photoelectrochemical cell employing the ferricenium/ferrocene couple.

The observation of a cathodic current peak in the dark at a potential more anodic than the photoanodic peak current is interesting. According to the simple model[8] for interfacial charge transfer processes at an n-type semiconductor, the cathodic current here should have its onset at the so-called flat band potential of the electrode, E_{fb}, and should peak at a potential more negative than E_{fb}. E_{fb} is that value of E_f where there is no band bending; see Scheme II. The prevailing rationale[9] for the observation of a reduction current at potentials more positive than E_{fb} is that there exist surface electronic levels which can be filled very rapidly with electrons and these filled levels overlap the distribution of unfilled states of the electrolyte solution.

The cyclic voltammetric scans in Figure 1a are repeatable and penwidth reproducibility has been achieved for greater than 30 cycles between −0.6 and +0.4 V vs SCE at 100 mV/s. These cyclic voltammetric data unequivocally show that ferrocene is oxidizable at illuminated n-type Si in competition with oxide formation.[6b] In the absence of ferrocene the cyclic voltammetric scans show a photoanodic current which declines on each successive scan. This photoanodic current apparently corresponds to oxide growth from traces of H_2O in the solution and there are no reduction waves over the potential range scanned.

Figure 1b shows the cyclic voltammetric behavior subsequent to the addition of Ar-purged, distilled H_2O to the solution used in Figure 1a. With every scan the photoelectrode properties deteriorate and after ten scans there is very little photooxidation current which corresponds to ferrocene oxidation. In this electrolyte solution containing ~6.9 M H_2O the $Si \rightarrow SiO_x$ conversion dominates the observed redox chemistry, and it is apparent that ferrocene oxidation cannot be sustained. The scans in Figure 1b show the typical effect of oxide growth: the photoanodic current onset shifts to more positive potentials and waves for solution species are significantly attenuated as the oxide grows.

B. Cyclic Voltammograms for Derivatized Si in EtOH Solutions of Ferrocene. The same electrode used in Figure 1 was reetched in HF and derivatized with (1,1′-ferrocenediyl)dichlorosilane as previously reported.[3] Figure 2a shows the cyclic voltammograms of the derivatized n-type Si in a dry EtOH solution of 0.1 M $[n\text{-}Bu_4N]ClO_4$. Bound, electroactive ferrocene moieties are present and durable, since persistent cyclic peaks (photoanodic and cathodic return) are observed at nearly the same potential as for naked Si in a solution containing ferrocene (Figure 1a). The properties of the derivatized electrode are quite similar to those previously reported:[3] the observation of anodic current requires illumination to generate holes, but reduction of the surface-bound oxidized material does not; the waves are persistent; and the waves are at a substantially more negative potential than on a Pt electrode.[10,11]

Illumination of the derivatized electrode in the "wet" electrolyte solution used in Figure 1b shows unequivocally that the derivatized electrode is more durable than the naked electrode in the same medium. Figure 2b shows that even after ten scans there is still excellent agreement with data for naked Si in a dry electrolyte solution (Figure 1a). Not only is the photooxidation of the solution ferrocene sustained, but also it occurs as efficiently as at the naked electrode in a dry solution, with respect to the position of peak potentials and the magnitude of the currents. Removing the electrode from the "wet" solution and redetermining the data in Figure 2a shows little loss of surface-attached material (Figure 2c).

It is evident that the derivatized electrode is substantially

more durable than a naked electrode in the "wet" ferrocene solution, but the derivatized electrode does undergo some minor changes as well. In Figure 2b it is evident that a process other than ferrocene oxidation obtains, since there is an increase in the current after the diffusion-limited ferrocene oxidation peak. This additional anodic current is very likely attributable to some amount of oxide growth. However, note that in Figure 2c the waves are in nearly the same position as in Figure 2a. This indicates that the oxide growth is not seriously undermining the derivatizing layer of the surface-attached reagent. Rather, it is very likely that the oxide growth occurs on areas of the exposed surface where there are pinholes in the derivatizing layer. Oxide likely grows on these underivatized regions and passivates them. Prolonged cycling of the electrode ultimately results in no apparent oxidation processes other than the oxidation of ferrocene. The effective electrode area passivated must be rather small, since the peak photoanodic current in Figure 2b is nearly the same as in Figure 1a. This similarity in photocurrent suggests that stabilization by derivatization does not necessarily mean sacrificing good quantum efficiency (vide infra).

C. Proof of Mediated Oxidation of Solution Species by Surface-Attached Electroactive Molecules. For an n-type semiconductor, the oxidation of the surface-attached molecule depends on potential *and light*. By definition, the oxidation of the surface-attached molecule on a reversible electrode, e.g., Pt, depends only on potential. The following experiments show that it is possible to exploit the two-stimuli response of the semiconductor in order to gain some direct evidence for mediated oxidation of a solution species.

Figure 3a shows the cyclic voltammetric characterization of a derivatized n-type Si electrode in a dry EtOH solution of 0.1 M $[n\text{-}Bu_4N]ClO_4$. Since the electroactive species corresponding to the observed waves are attached to the electrode, the curves shown are the same in stirred or quiet solutions. Figure 3b shows the current–potential plot for the derivatized electrode in the presence of a ferrocene electrolyte solution. Note that the current is much larger than in Figure 3a but still gives a diffusion-limited peak for the quiet solution. As usual, the reduction current peak is more anodic if the light is switched off at the anodic limit, since there is no competing hole process. The key result is that, when the solution is stirred and the light is switched off at the anodic limit, there is only a very small cathodic current for the reduction of the surface-attached oxidant. That is, the surface-attached oxidant has been reduced by solution ferrocene species, and the oxidized products are swept away from the electrode by stirring to preclude the observation of the reduction current. Upon stirring the photoanodic current increases to a light intensity (hole) limited current, as expected.

By switching off the light near the anodic limit of the scan one ceases to create new, oxidized, surface-attached species. The return scan then allows a measure of the photogenerated surface-attached oxidant as was done in Figures 3a or 2a. In the presence of a solution reductant the surface-attached oxidant can be reduced at a rate which is competitive with the scan time along the potential axis. For the reversible electrode the amount of surface-attached oxidant at any time only depends on the potential, and the reduction of the surface-attached oxidant by a solution species will not be directly measurable by cyclic voltammetry.

The data in Figure 2b were repeated ten times with the same electrode and afterward the electrode was shown to retain >85% of its original surface-attached electroactive material. Data of this sort have allowed a conservative estimate of $>10^4$ turnovers per attached electroactive ferrocene center without deterioration of the properties of the derivatized electrode in the dry EtOH solution.

D. Use of Derivatized Si in H_2O Solution. Photooxidation of Ferrocyanide. The results for naked vs. derivatized Si in EtOH solutions with H_2O present (Figure 1b vs. 2b) encouraged us to attempt the use of n-Si in aqueous electrolytes. Derivatized n-type Si does exhibit well-defined, persistent cyclic voltammetric waves in aqueous electrolytes. For pHs between 0 and 6 the electrodes are very durable and seem to

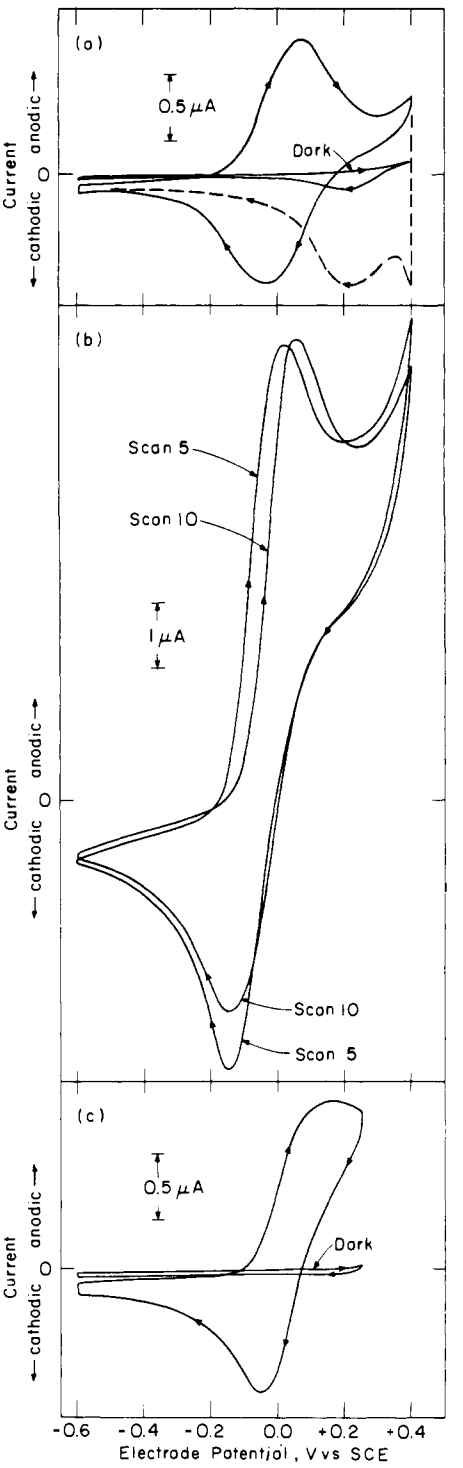

Figure 2. (a) Cyclic voltammograms for n-type Si used in Figure 1 derivatized with (1,1′-ferrocenediyl)dichlorosilane in 0.1 M $[n\text{-}Bu_4N]ClO_4$/EtOH at 100 mV/s. One scan is shown for total darkness; the smooth scan with peaks at +0.08 and −0.05 V is with illumination; where the dashed curve begins (~+0.4 V) the illumination was blocked to show the cathodic peak position in the dark. (b) Cyclic voltammograms (scans 5 and 10) using the derivatized electrode in the solution used in Figure 1b. All conditions are the same as in Figure 1b except that the electrode is derivatized. (c) Repeat of Figure 2a with illumination showing that the derivatized surface is intact after scans in Figure 2b.

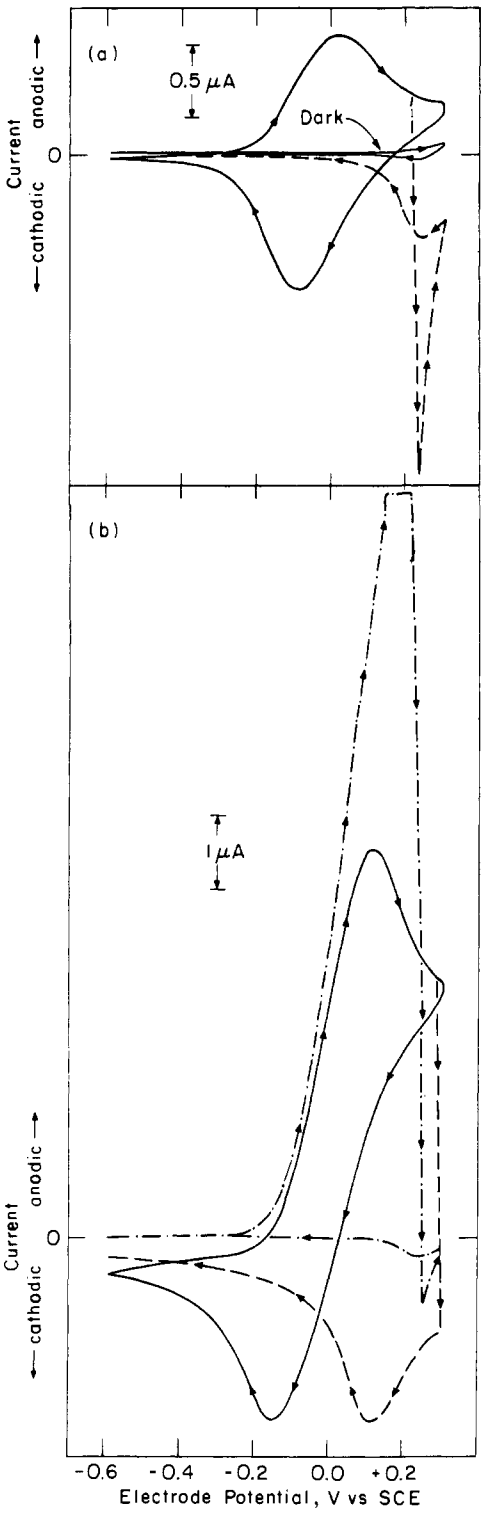

Figure 3. (a) Cyclic voltammograms for another derivatized n-type Si electrode in 0.1 M [n-Bu_4N]ClO_4/EtOH as in Figure 2a. The curves are the same upon stirring the electrolyte solution. (b) Cyclic voltammograms for the derivatized electrode in the same solution plus 5×10^{-4} M ferrocene: (—) with illumination of electrode, quiet solution; (- - -) with illumination blocked at +0.3 V, quiet solution (- · - ·) with illumination blocked at +0.22 V, stirred solution.

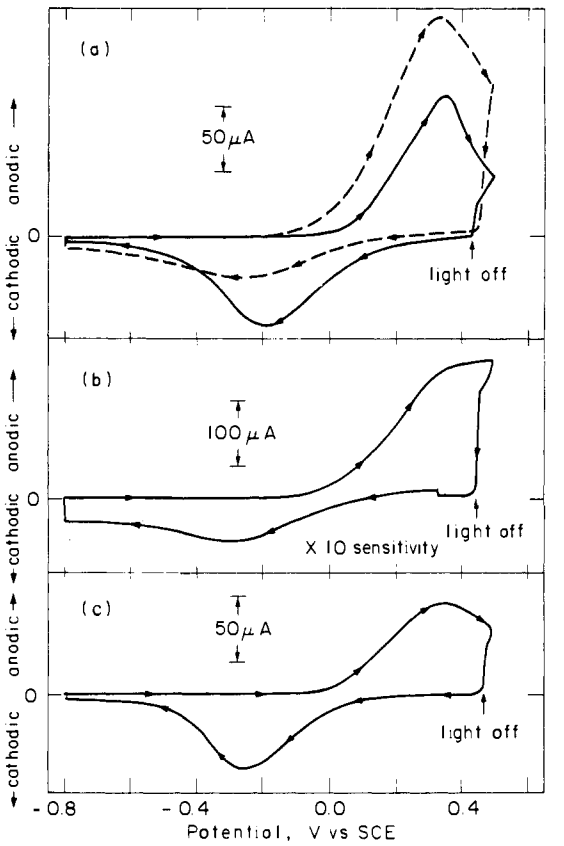

Figure 4. Cyclic voltammograms at 100 mV/s of n-type Si derivatized with (1,1′-ferrocenediyl)dichlorosilane in aqueous electrolytes. The electrode is illuminated with a tungsten halogen source during the anodic scans; the cathodic, return scans are in the dark. (a) Cyclic voltammograms in quiet solutions: (—) 0.1 M $NaClO_4/H_2O$ showing surface waves at +0.3 (photooxidation) and −0.1 V (reduction), (- - -) with 9×10^{-4} M $K_4Fe(CN)_6$ added. (b) The effect of stirring on cyclic voltammogram in 9×10^{-4} M $K_4Fe(CN)_6$ electrolyte. Note that the reverse scan current scale is expanded by 10 times the forward scan scale. (c) Repeat of (a) (—) after completion of (b).

be more so for the lower pHs. Alkaline solutions have been avoided owing to the known degradation of ferricenium in alkaline solution.[12]

We have demonstrated the mediated oxidation of $Fe(CN)_6^{4-}$ in aqueous solution (Figure 4). In Figure 4a the cyclic voltammograms for a derivatized electrode in a quiet aqueous electrolyte solution with and without $Fe(CN)_6^{4-}$ are shown. Note that upon the addition of $Fe(CN)_6^{4-}$ the photoanodic current peak is larger while the reduction current is attenuated. The solution oxidation product, $Fe(CN)_6^{3-}$, is only sluggishly reduced at the derivatized electrode surface and even at naked n-type Si the reduction of $Fe(CN)_6^{3-}$ is sluggish compared to Pt, for example. Stirring the electrolyte solution containing $Fe(CN)_6^{4-}$ results in an even larger photoanodic current which is no longer diffusion limited, and the reduction peak corresponding to surface-attached oxidant is nearly completely diminished. The $E°$ for the $Fe(CN)_6^{3-}/Fe(CN)_6^{4-}$ [13] system is +0.2 V vs. SCE, and we have observed sustained oxidation currents at modestly contrathermodynamic potentials, but the demonstrated energy conversion efficiency is low owing to the low output potentials (vide infra).

The data in Figure 4 show that the derivatized Si photoelectrode can be used to effect oxidation reactions in aqueous electrolytes and that a large fraction of the observed photocurrent is in fact mediated oxidation of the solution species. The particular electrode illustrated in Figure 4 is one which has a polymeric amount of electroactive material attached to the surface. The surface coverage is $\sim 10^{-9}$ mol/cm^2 of exposed Si area from the integrated area under the photoanodic peak. Smaller coverages are persistent in aqueous solutions but qualitatively require the lower pHs for durability.

Illuminated naked n-type Si in aqueous electrolytes appears to give some $Fe(CN)_6^{4-}$ oxidation, but at concentrations of $Fe(CN)_6^{4-}$ similar to that in Figure 4 the electrode is rapidly passivated by oxide growth. Under no conditions have we been

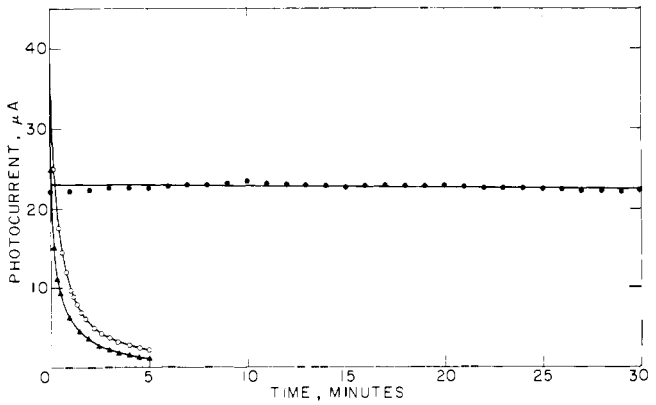

Figure 5. Plots of photocurrent against time for a single n-Si electrode illuminated with 632.8-nm light at ~6 mW. Photoelectrode held at +0.2 V vs. SCE in stirred solutions. Supporting electrolyte is 0.1 M $NaClO_4$ in doubly distilled, deionized H_2O. Run 1 (▲), HF-etched "naked" electrode in supporting electrolyte only. Run 2 (○), "naked" electrode reetched with HF, in supporting electrolyte plus 4×10^{-3} M $Fe(CN)_6^{4-}$. Run 3 (●), electrode derivatized with (1,1′-ferrocenediyl)dichlorosilane in same solution as run 2.

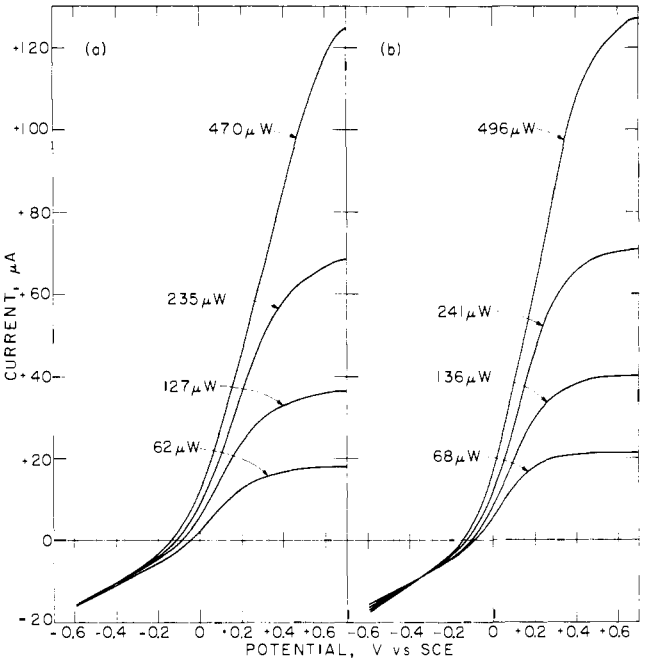

Figure 6. Current-voltage curves at 2 mV/s for n-Si photoelectrode in stirred EtOH solution of 5×10^{-2} M ferrocene, 2.9×10^{-3} M ferricenium as the PF_6^- salt, and 0.1 M $[n\text{-}Bu_4N]ClO_4$. Uniform irradiation with 632.8-nm light at the indicated power. Solution E_{redox} = +0.32 V vs. SCE. Part (a), "naked" electrode freshly etched with HF; part (b), same electrode after derivatization with (1,1′-ferrocenediyl)dichlorosilane. See also Table I.

able to observe well-defined, diffusion-limited oxidation waves for $Fe(CN)_6^{4-}$ at illuminated naked n-type Si, in contrast to the situation for derivatized electrodes. Figure 5 shows the photocurrent vs. time for a naked n-Si electrode compared to a derivatized electrode in an aqueous electrolyte solution containing $Fe(CN)_6^{4-}$. The improvement in the maintenance of a constant photocurrent for the derivatized electrode is obvious. Ultimately, the derivatized electrode suffers deterioration of its properties as well, but $>10^3$ electrons per electroactive ferrocene can be passed through the interface without significant (<10%) decline in the photocurrent. There is a general decline in the amount of attached electroactive material with prolonged passage of photocurrent.

E. Equilibrium Current-Potential Curves. In order to assess the practical aspects of a derivatized electrode in a photoelectrochemical device we have determined equilibrium current-potential curves for the derivatized n-type Si under conditions where comparison with the naked electrode is possible. From such curves one can assess optical to electrical energy conversion efficiency for cases where the light intensity is known. Figure 6 shows a comparison of the current-potential characteristics of naked Si- and derivatized Si-based photoelectrochemical cells employing a dry EtOH electrolyte solution containing the ferricenium/ferrocene couple. Output characteristics are given in Table I. The data show that output characteristics for the cell employing the derivatized electrode are as good as, if not better than, those obtained with the naked electrode. The data reported here are comparable to those reported previously for the naked Si-based cells.[6] The overall efficiencies are low and decline at the higher intensities. The major problem is a low open-circuit photopotential at low intensity and worsening fill factors as the light intensity is increased. But the main point here is that the properties are not worsened by the derivatization procedure. The derivatized electrode appears to be more efficient, especially at the lowest intensity, but the effects are not dramatic. The data in Figure 6 were repeated two times in independent experiments with essentially the same results. In these experiments the properties of the derivatized electrode were nearly the same before and

Table I. Representative Output Characteristics for n-Type Si-Based Photoelectrochemical Cells[a]

electrode	input, μW[b]	Φ_e[c]	max power output, μW	max V (V at η_{max})[d], mV	η_{max}, %[e]
A. EtOH, 0.1 M $[n\text{-}Bu_4N]ClO_4$, 5×10^{-2} M Ferrocene, 2.9×10^{-3} M Ferricenium (E_{redox} = +0.32 V vs. SCE)					
"naked"	62	0.49	1.76	360 (190)	2.8
	127	0.47	3.24	410 (185)	2.6
	235	0.43	4.62	430 (165)	2.0
	470	0.29	5.94	450 (165)	1.3
"derivatized"	68	0.58	2.77	400 (205)	4.1
(coverage ≈ 6×10^{-9}	136	0.52	4.16	420 (180)	3.1
mol/cm²)	241	0.49	6.01	440 (185)	2.5
	496	0.36	8.08	460 (165)	1.6
B. H_2O, 0.1 M $Fe(CN)_6^{4-}$, 0.01 M $Fe(CN)_6^{3-}$ (E_{redox} = +0.13 V vs. SCE)					
"derivatized"	28.3	0.42	0.40	210 (110)	1.4
(coverage ≈ 7×10^{-9}	120	0.38	1.28	265 (100)	1.1
mol/cm²)	591	0.22	2.85	285 (100)	0.5
	1280	0.11	2.97	290 (90)	0.2

[a] Data are from curves shown in Figures 6 and 7. [b] Input power is from a 632.8-nm He-Ne laser. For power density multiply by 13 cm^{-2} for electrode in part A; multiply by 26 cm^{-2} for electrode in part B. [c] Quantum yield for electron flow at E_{redox}; this corresponds to the short-circuit quantum yield measured as the number of electrons passed per incident photon. [d] Maximum voltage is the open-circuit photopotential and the value in parentheses is the output voltage at the maximum power point. [e] Efficiency for conversion of 632.8-nm light to electricity.

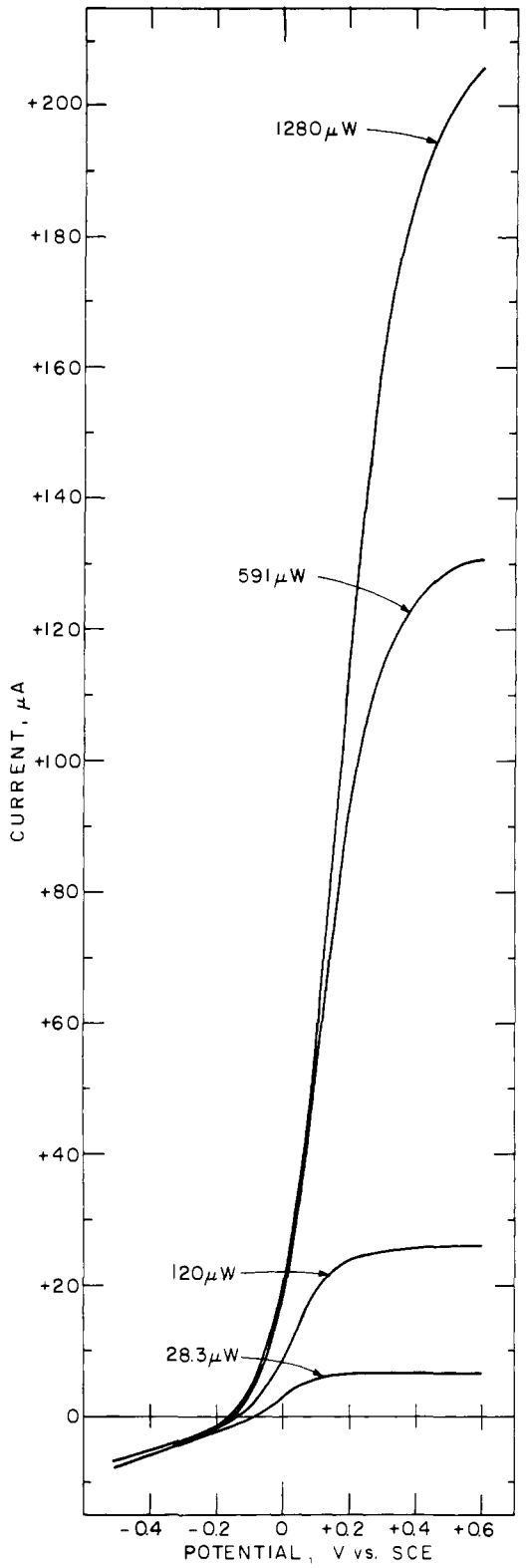

Figure 7. Current-voltage curves for n-Si photoelectrode derivatized with (1,1′-ferrocenediyl)dichlorosilane in stirred 0.1 M $Fe(CN)_6^{4-}$, 0.01 M $Fe(CN)_6^{3-}$, in doubly distilled, deionized H_2O. n-Si illuminated at 632.8 nm at the indicated power. Solution E_{redox} = +0.13 V vs. SCE; scan rate 5 mV/s. See also Table I.

after recording the current-potential curves. Coverage of electroactive material was invariant within 2%.

Figure 7 shows equilibrium current-potential curves for a derivatized Si-based photoelectrochemical cell employing an H_2O solution of $Fe(CN)_6^{3-}/Fe(CN)_6^{4-}$ with E_{redox} at +0.13 V vs. SCE. Such curves could not be recorded at all for a naked Si-based cell, since the surface undergoes decomposition on the time scale of one scan. A summary of the output properties of the cell is included in Table I. The data show that it is possible to effect light to electrical energy conversion, but again the efficiencies are low. The short-circuit quantum yields are high, but the output potential and fill factor are poor as in Figure 6.

Summary

The experiments described herein illustrate some of the potential utility of molecular derivatization of semiconductor photoelectrodes. The data adequately show that n-type Si can be substantially protected from deleterious SiO_x growth under illumination in H_2O containing electrolyte solutions. The change in current efficiency for SiO_x growth is a consequence of change in relative rates of interfacial charge transfer processes. Manipulation of the kinetics is likely attributable in part to the physical protection of the surface of the Si by the derivatizing layer of ferrocene material, but this point needs further study. Further, derivatization appears to result in photosensitive surfaces with output parameters (potential, current) which can be as good as the naked Si in dry electrolyte solution. Finally, the n-type semiconductor has a response to two stimuli (light and potential) with respect to oxidation processes and has allowed the first direct proof of mediated electron transfer at a derivatized electrode of any kind. Mediated oxidation of ferrocene in EtOH and $Fe(CN)_6^{4-}$ in H_2O solution has been demonstrated. Derivatized electrodes have been prepared which pass $>10^4$ electrons per electroactive site without deterioration of properties.

Experimental Section

Electrodes. Single-crystal, n-type Si wafers (0.25 mm thick, 111 face) doped with Sb and with resistivity of 4-5 Ω cm were obtained from General Diode Co., Framingham, Mass. The wafers were cut into pieces of area ~0.3 cm^2 and mounted as electrodes as previously reported.[6b] The back surface was rubbed with a Ga-In eutectic and secured with conducting Ag epoxy to a coiled Cu wire. The Cu wire lead was passed through a glass tube, and all surfaces were insulated with ordinary epoxy so as to leave only the front surface of the semiconductor exposed.

Before use, all electrodes were first etched in concentrated HF and rinsed with distilled H_2O. Electrodes to be used as "naked" electrodes were then rinsed in acetone and air dried; however, electrodes which were to be derivatized were immersed for 60 s in 10 M NaOH, before rinsing with distilled H_2O and acetone.

For derivatization, the electrodes were exposed for 1-3 h to a solution of $\sim 10^{-2}$ M (1,1′-ferrocenediyl)dichlorosilane[3,10b] in Ar-purged isooctane (298 K) under an Ar atmosphere. The electrodes were then rinsed in isooctane and in absolute EtOH and used in photoelectrochemical cells.

Chemicals. Reagent grade $K_3[Fe(CN)_6]$, $K_4[Fe(CN)_6]\cdot 3H_2O$, and anhydrous $NaClO_4$ were used as received from commercial sources. Polarographic grade $[n\text{-}Bu_4N]ClO_4$ (Southwestern Analytical Chemicals) was dried in an oven for several days prior to use, and reagent-quality ferrocene was further purified by sublimation. Absolute EtOH and spectroquality isooctane were used without further purification.

Electrochemical Characterization. All experiments were performed in single-compartment Pyrex vessels equipped with a saturated calomel (SCE) reference electrode, Pt wire cathode, and Si photoanode. The supporting electrolytes were either 0.1 M $[n\text{-}Bu_4N]ClO_4$ in absolute EtOH or 0.1 M $NaClO_4$ in distilled H_2O; however, for experiments in 0.1 M $Fe(CN)_6^{4-}$, no supporting electrolyte was necessary owing to the already high ionic concentration. Cyclic voltammograms and equilibrium current-voltage curves were obtained using a PAR 173 potentiostat equipped with a Model 179 coulometer and driven by a Model 175 voltage programmer. Traces were recorded on a Houston Instruments *XY* recorder, or, for current vs. time plots, on a Hewlett-Packard strip chart recorder. A 500-W tungsten-halogen lamp was used for cyclic voltammograms with $Fe(CN)_6^{4-}$; for all other experiments, uniform irradiation of ~3 mW at 632.8 nm was

provided by a He-Ne laser. Laser intensity was varied with Corning colored glass filters and monitored with a beam splitter and a Tektronix J16 digital radiometer equipped with J6502 probe. The laser beam was masked to match the size of the Si surface.

For experiments involving switching between different solutions (e.g., with and without ferrocene), the various solutions were prepared in advance in separate Pyrex cells using a common sample of supporting electrolyte. The interchange of solutions was effected by first disconnecting the potentiostat leads and then, with all electrodes clamped in place, removing the initial cell, rinsing the electrodes in a beaker of pure solvent, and then securing the new solution-containing cell in position. The controlled addition of H_2O to ferrocene-EtOH solutions was accomplished by disconnecting the potentiostat leads and injecting by syringe a premeasured aliquot of distilled H_2O. The solution was stirred briefly by a magnetic stir bar, and the voltammetric scans were then resumed.

Electrodes destined for use in aqueous solution first had their cyclic voltammetric properties recorded in 0.1 M $[n\text{-}Bu_4N]ClO_4$-EtOH immediately after derivatization. The electrodes were then transferred to a cell containing 0.1 M $NaClO_4$ in doubly distilled deionized H_2O. For cyclic voltammetric studies (Figure 4), the electrodes were scanned several times until their voltammetric behavior had stabilized; for current vs. time studies (Figure 5), the electrodes were instead irradiated while at +0.2 V vs. SCE until the anodic current due to oxidation of surface-attached material had declined to less than 0.5 μA. Following this preliminary procedure, the $Fe(CN)_6^{4-}$ was introduced by pipet or syringe injection of a measured amount of $Fe(CN)_6^{4-}$ stock solution. In the current against time plots, mediated electron transfer to $Fe(CN)_6^{4-}$ was thereby initiated, and the photocurrent immediately assumed, and maintained, the value shown in Figure 5.

For equilibrium current-potential curves in aqueous $Fe(CN)_6^{4-}$ (Figure 7), the electrodes were derivatized and checked in 0.1 M $[n\text{-}Bu_4N]ClO_4$-EtOH as above. However, they were then transferred directly to a cell containing 0.1 M $Fe(CN)_6^{4-}$ and 0.01 M $Fe(CN)_6^{3-}$ in doubly distilled, deionized water, without preliminary cycling in 0.1 M $NaClO_4$-H_2O.

Acknowledgments. We thank the U.S. Department of Energy, Office of Basic Energy Sciences, for support of this research. M.S.W. acknowledges support as a Dreyfus Teacher-Scholar grant recipient, 1975-1980, and N.S.L. acknowledges support as a John and Fannie Hertz Foundation Fellow, 1977-present.

References and Notes

(1) A. J. Bard and M. S. Wrighton, *J. Electrochem. Soc.*, **124**, 1706 (1977).
(2) H. Gerischer, *J. Electroanal. Chem.*, **82**, 133 (1977).
(3) M. S. Wrighton, R. G. Austin, A. B. Bocarsly, J. M. Bolts, O. Haas, K. D. Legg, L. Nadjo, and M. C. Palazzotto, *J. Am. Chem. Soc.*, **100**, 1602 (1978).
(4) M. Fujihira, N. Ohishi, and T. Osa, *Nature (London)*, **268**, 226 (1977).
(5) W. D. K. Clark and N. Sutin, *J. Am. Chem. Soc.*, **99**, 4676 (1977), and references cited therein.
(6) (a) M. S. Wrighton, J. M. Bolts, A. B. Bocarsly, M. C. Palazzotto, and E. G. Walton, *J. Vac. Sci. Technol.*, **15**, 1429 (1978); (b) K. D. Legg, A. B. Ellis, J. M. Bolts, and M. S. Wrighton, *Proc. Natl. Acad. Sci. U.S.A.*, **74**, 4116 (1977).
(7) G. J. Janz and R. P. T. Tomkins, "Nonaqueous Electrolytes Handbook", Vol. II, Academic Press, New York, 1973, and references cited therein.
(8) H. Gerischer in "Physical Chemistry: An Advanced Treatise", Vol. 9A, H. Eyring, D. Henderson, and W. Jost, Eds., Academic Press, New York, 1970, Chapter 5.
(9) (a) P. A. Kohl and A. J. Bard, *J. Am. Chem. Soc.*, **99**, 7531 (1977); (b) S. N. Frank and A. J. Bard, *ibid.*, **97**, 7427 (1975).
(10) (a) M. S. Wrighton, R. G. Austin, A. B. Bocarsly, J. M. Bolts, O. Haas, K. D. Legg, L. Nadjo, and M. C. Palazzotto, *J. Electroanal. Chem.*, **87**, 429 (1978); (b) M. S. Wrighton, M. C. Palazzotto, A. B. Bocarsly, J. M. Bolts, A. B. Fischer, and L. Nadjo, *J. Am. Chem. Soc.*, **100**, 7264 (1978).
(11) A. Merz and A. J. Bard, *J. Am. Chem. Soc.*, **100**, 3222 (1978).
(12) E. Becker and M. Tsutsui, Eds., "Organometallic Reactions", Vol. IV, Wiley, New York, 1972, pp 356-357.
(13) I. M. Kolthoff and W.J. Tomsicek, *J. Phys. Chem.*, **39**, 945 (1935).

Mechanistic Studies of Arene Oxide and Diol Epoxide Rearrangement and Hydrolysis Reactions

J. E. Ferrell, Jr., and G. H. Loew*

Contribution from the Molecular Theory Laboratory, Genetics Department, Stanford University Medical School, Stanford, California 94305. *Received June 15, 1978*

Abstract: Using the semiempirical all valence electron MINDO/3 method, the mechanisms of acid-catalyzed rearrangement and hydrolysis of benzene oxide and benzene diol epoxide were studied. Both product stabilities and reaction pathways were calculated. The results show that benzene oxide prefers phenol formation to hydrolysis, and suggest that the mechanism for this reaction involves rate-determining S_N1-type formation of a carbocation quickly followed by the NIH shift, in agreement with experiment. Formation of a carbocation in benzene diol epoxide is less favorable, and should also be followed by the NIH shift leading to a ketone. Since this sort of ketone is only a minor product of the diol epoxides studied to date, it is inferred that the hydrolysis of benzene diol epoxide does not proceed by carbocation trapping, but instead by an S_N2 mechanism. These results are used to rationalize why polycyclic diol epoxides are highly mutagenic and good candidates as ultimate carcinogens, whereas polycyclic arene oxides are not.

Introduction

In 1950 Boyland suggested that arene oxides are formed as intermediates in the metabolism of polycyclic aromatic hydrocarbons.[1] Subsequent work by Jerina established that naphthalene is metabolized to 1-naphthol via an arene oxide intermediate, and demonstrated what has become the hallmark of such reactions: a Whitmore 1,2 shift[2] related to the familiar pinacol rearrangement[3] and now called the NIH shift.[4] Arene oxides have now been implicated in the formation of phenols, diols, ketones, glutathione conjugates, and other important metabolites of polycyclic aromatic hydrocarbons.[5]

Recently, much attention has been paid to the formation and reactions of arene oxides as a result of interest in the bay region hypothesis. As illustrated below, it is now thought that the activation of polycyclic aromatic hydrocarbons to ultimate carcinogens requires three steps: initial epoxidation by the P-450 monooxygenases, followed by epoxide hydrase mediated hydrolysis, and a second epoxidation. This yields a diol epoxide which can interact with tissue nucleophiles including DNA. The bay region hypothesis is supported by observations on benz[*a*]anthracene,[6] 7-methylbenz[*a*]anthracene,[7] benzo[*a*]pyrene,[8] 3-methylcholanthrene,[9] dibenz[*a*,*h*]anthra-

0002-7863/79/1501-1385$01.00/0